Mortality Prediction in Severe Congestive Heart Failure Patients With Multifractal Point-Process Modeling of Heartbeat Dynamics

Gaetano Valenza, Herwig Wendt, Ken Kiyono, Junihiro Hayano, Eiichi Watanabe, Yoshiharu Yamamoto, Patrice Abry, Riccardo Barbieri

Mortality Prediction in Severe Congestive Heart Failure Patients With Multifractal Point-Process Modeling of Heartbeat Dynamics

Gaetano Valenza, *Member, IEEE*, Herwig Wendt, *Member, IEEE*, Ken Kiyono, Junichro Hayano, Eiichi Watanabe, Yoshiharu Yamamoto, *Member, IEEE*, Patrice Abry, *Fellow, IEEE*, and Riccardo Barbieri, *Senior Member, IEEE*

Abstract*—*Background: **Multifractal analysis of human heartbeat dynamics has been demonstrated to provide promising markers of congestive heart failure (CHF). Yet, it crucially builds on the interpolation of *RR* interval series which has been generically performed with limited links to CHF pathophysiology. *Objective:* We devise a novel methodology estimating multifractal autonomic dynamics from heartbeat-derived series defined in the continuous time. We hypothesize that markers estimated from our novel framework are also effective for mortality prediction in severe CHF. *Methods:* We merge multifractal analysis within a methodological framework based on inhomogeneous point process models of heartbeat dynamics. Specifically, wavelet coefficients and wavelet leaders are computed over measures extracted from instantaneous statistics of probability density functions characterizing and predicting the time until the next heartbeat event occurs. The proposed approach is tested on data from 94 CHF patients aiming at predicting survivor and nonsurvivor individuals as determined after a four years follow up. *Results and Discussion:* Instantaneous markers of vagal and sympatho-vagal dynamics display power-law scaling for a large range of scales, from $\simeq 0.5$ to $\simeq 100$ s. Using standard support vector machine algorithms, the proposed inhomogeneous point-process representation-based multifractal analysis achieved the best CHF mortality prediction accuracy of 79.11% (sensitivity 90.48%, specificity 67.74%). *Conclusion:* Our results suggest that heartbeat scaling and multifractal properties in CHF patients are not generated at the sinus-node level, but rather by the intrinsic action of vagal short-term control and of sympatho-vagal fluctuations associated with circadian cardiovascular control especially within the very low frequency band. These markers might provide crit-ical information in devising a clinical tool for individualized prediction of survivor and nonsurvivor CHF patients.**

***Index Terms*—Multifractal analysis, point process, heart rate variability, wavelet coefficients, wavelet leaders, congestive heart failure, autonomic nervous system.**

I. Introduction

NONLINEAR dynamics of human cardiovascular oscillations has long been recognized throughout the past two decades [1]–[3]. In fact, because of the multiple dynamical interplay with other physiological systems (e.g., endocrine, neural, and respiratory), as well as multiple biochemical processes, combined sympathetic and vagal stimulations on heart rate control are not simply additive [1]. Consequently, standard estimates from heartbeat dynamics defined in the time and frequency domains [4], which intrinsically assume that the magnitude of cardiac responses is proportional to the strength/amplitude of the autonomic stimuli, need complementary nonlinear/multiscale metrics (see [2], [4]–[6] and references therein for reviews). Among others, fractal theory has been giving a major contribution in understanding complex cardiovascular dynamics especially involving nonlinear cardiovascular control and related autonomic nervous system (ANS) activity [2], [5], [7]–[11]. Recently, a robust and efficient procedure relying on the use of multiscale representation and wavelet leaders, has been proposed to conduct multifractal analysis [10] and tested on heartbeat series [8], [11].

A paradigmatic clinical application of these metrics refers to severe congestive heart failure (CHF) [9], [12]. Indeed, nonlinear measures derived from bispectral, entropy, and non-Gaussian analyses have been proven effective in discerning healthy subjects from CHF patients at a group-wise level [2], [4], [5], [12]–[17]. Also in CHF patients, departures from Gaussianity were used to evaluate increased mortality risk [9], and compared against fractal exponent [18]. Leveraging on the so-called cardiovascular fractal complexity at many spatial and temporal scales, multifractal analyses were successfully employed to model ANS regulatory actions and related temporal

This work was supported in part by Grant ANR-16-CE33-0020 MultiFracs and Grant CNRS PICS 7260 MATCHA. *(Corresponding author: Gaetano Valenza.)*

G. Valenza is with the Computational Physiology and Biomedical Instruments group at the Bioengineering and Robotics Research Center E. Piaggio & Department of Information Engineering, University of Pisa, Pisa 56126, Italy (e-mail: g.valenza@ieee.org).

H. Wendt is with IRIT, Universit. de Toulouse, CNRS.

K. Kiyono is with the Osaka University.

J. Hayano is with the Graduate School of Medical Science, Department of Medical Education, Nagoya City University.

E. Watanabe is with the Department of Cardiology, Fujita Health University School of Medicine.

Y. Yamamoto is with the Graduate School of Education, The University of Tokyo, Tokio, Japan.

P. Abry is with the Physics Department, ENS Lyon, CNRS.

R. Barbieri is with the Department of Electronics, Informatics and Bioengineering, Politecnico di Milano.

Digital Object Identifier 10.1109/TBME.2018.2797158

fluctuations in CHF heartbeat dynamics [2], [4], [5], [19], [20]. Additionally, in discerning the healthy from CHF patients, Dutta [21] reported on the dependency of parameters on multifractal spectra, whereas Galaska *et al.* [22] pointed on advantages of multifractal detrended fluctuation analysis.

Nevertheless, several limitations can be pointed out in dealing with current multiscale approaches: i) the intrinsic discrete nature of the unevenly sampled R-R interval series can lead to estimation errors; considering the series as inter-events does not allow for matching time scales, and may be missing intrinsic generative properties as reflected in complex dynamics; ii) the application of preliminary interpolation procedures could affect complexity estimates, with a bias from the specific interpolation function (e.g., linear, polynomial, etc.); iii) multifractal analysis has always been performed over series of heartbeat dynamics exclusively; therefore it is unknown whether scale-free properties arise from the nonlinear/complex interactions between sympathetic and parasympathetic activity at the level of the sinoatrial node (as thoroughly reported in [1]), or whether there are already intrinsic multifractal properties in each autonomic dynamics *per se*; iv) specifically for CHF, an effective prediction of mortality risk, as well as risk stratification, at a single-subject level with enough accuracy for a direct application in clinical practice [9], [11], [23], [24] is still missing.

Acronym	
ANS	Autonomic Nervous System
CHF	Congestive Heart Failure
ECG	Electrocardiogram
LF	Low Frequency
LOO	Leave one out
HF	High Frequency
HR	Heart Rate
NS	Non-Survivors
PDF	Probability Density Function
RFE	Recursive Feature Elimination
SV	Survivors
SVM	Support Vector Machine
VLF	Very Low Frequency

To overcome these limitations, in this study we propose a novel methodology combining multifractal analysis and inhomogeneous point-process models, which have been specifically devised for cardiovascular dynamics [14], [25]. Specifically, we propose multiscale representation and the so-called wavelet p-leaders, i.e., local ℓ^p norms of wavelet coefficients [10], [26] of moments derived from probability density functions (PDFs) characterizing and predicting the time until the next heartbeat event occurs. To this extent, we proposed the use of inhomogeneous point-processes to effectively characterize the probabilistic generative mechanism of heartbeat events, even considering short recordings under nonstationary conditions [25]. The unevenly spaced heartbeat intervals are then represented as multiscale quantities of a state-space point process model defined at each moment in time, thus allowing to estimate instantaneous measures without using any interpolation method, therefore overcoming limitations i) and ii). We demonstrate how to capture fluctuations of regularity in heartbeat data by scanning all details finer than the chosen analysis scale [8], [11]. To compare our method against a more standard approach, we also investigate the use of a non-informative standard spline-based interpolation. Finally, we here study multiscale properties of heartbeat-derived series with high resolution in time, including long-term instantaneous mean heart rate, standard deviation, and low-frequency (LF) and high-frequency (HF) spectral powers, which correspond to time-varying vagal activity estimates [4], thus overcoming limitation iii). Application of these metrics is then performed on experimental data gathered from 94 CHF patients by evaluating the recognition accuracy in predicting survivor and non-survivor patients after a 4 years follow up, demonstrating how to overcome limitation iv). Of note, preliminary results associated with this study were presented in [27], [28], in which a wavelet leader-based multiscale representation was applied to instantaneous heartbeat series as well as to instantaneous vagal activity series. Here, we significantly expand on these results by generalizing the development of the methodology to be suitable for generic inhomogeneous point process-derived heartbeat dynamics series defined in continuous time, as well as by increasing the number of patients involved in the experiment, and accounting for their clinical characteristics. Furthermore, the scale dependent features resulting from the proposed methodology have been exploited through nonlinear support vector machines and related feature selection procedures.

II. Materials and Methods

In this Section, we provide theoretical and methodological details on the proposed multifractal approach for inhomogeneous point-processes of heartbeat dynamics. The overall processing chain is shown in Fig. 1. Specifically, automatic R-peak detection is performed on artifact-free ECG series from each CHF patient enrolled in this study. Recognition and correction of eventual algorithmic (e.g., R-peak mis-detection) and/or physiological artifacts (e.g., ectopic beats) was performed through our recently proposed log-likelihood point process-based method [29]. Then, for each *RR* interval series from each subject, a continuous PDF in time, in the form of inverse-Gaussian distribution, is estimated for each heartbeat event considering the long-term past events. From such continuous PDFs, multiscale representations of a number of instantaneous estimates defined in the time (e.g., mean heart rate and standard deviation) and frequency domains (e.g., LF and HF powers) are derived. Finally, these and further features are fed into a standard Support Vector Machine (SVM) to predict mortality in CHF patients at a single-

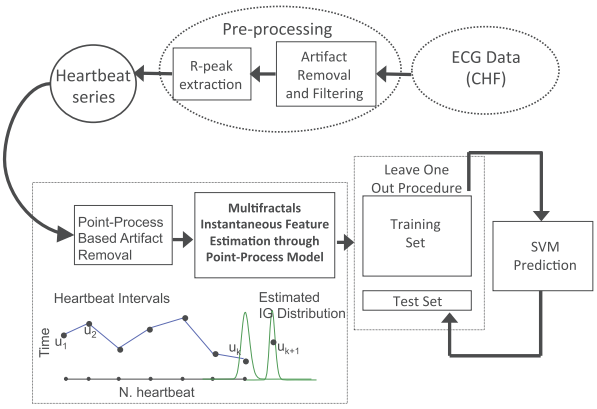

Fig. 1. Overall data processing chain.

subject level. Validation was performed through a leave-one-out procedure. Mathematical details of each processing stage follow below.

TABLE I
BASELINE CLINICAL CHARACTERISTICS OF THE PATIENTS

	Survivors ($n = 63$)	Non Survivors ($n = 31$)	p-val
Age [years]	66.5 ± 10	71 ± 8	>0.05
Sex [M/F]	39/24	17/14	>0.05
NYHA:			
class II	9(15.5%)	3(9.7%)	>0.05
class III–IV	54(84.5%)	28(90.3%)	>0.05
Ischemia	15 (25.8%)	15(48.4%)	<0.05
LVEF [%]	36.5 ± 11.5	40 ± 10	>0.05
BNP [pg/mL]	483.5 ± 322.5	960.0 ± 490.0	<0.01
BUN [mg/dL]	18.5 ± 5.5	25.0 ± 8.0	<0.01
Cr [mg/dL]	0.8 ± 0.3	1.0 ± 0.4	<0.05
Beta-blocker	21(36.2%)	7(22.6%)	>0.05
Hb	12.25 ± 1.25	10.9 ± 1.9	<0.05
ACE/ARB	25(43.1%)	16(51.6%)	>0.05
Loop diuretic	26(44.8%)	21(67.8%)	<0.05
Spironolactone	14(24.1%)	13(41.9%)	<0.05
VPBh	1.062 ± 1.062	1.333 ± 1.333	>0.05

Uncorrected p-values calculated from Mann-Whitney Non-parametric tests for continuous variables and Chi-square test for other variables.
NYHA: New York Heart Association functional class; LVEF: Left ventricular ejection fraction; ACE: angiotensin-converting enzyme inhibitor; ARB: angiotensin II receptor blocker; BNP: brain natriuretic peptide; BUN: blood urea nitrogen; Cr: creatinine; Hb: Hemoglobin; VPBh: Ventricular premature beats per hour.

A. Experimental Data

24-hour Holter ECG recordings from a cohort of 94 patients suffering from CHF were made available by the Fujita Health University Hospital, Japan. Of these patients, 31 died within 33 ± 17 months (range, 1–49 months) after hospital discharge, whereas 61 survived for a longer time. The former group is referred to as non-survivors (NS) and the latter as survivors (SV). Further clinical details can be found in [9]. For each patient, R peak arrival times were carefully extracted from 24-hour Holter ECG recordings. Missing data and outliers stemming from atrial or ventricular premature complexes were handled by our preprocessing automated tools [29]. All *RR* interval series were also checked by visual inspection analysis. Subjects with sustained tachyarrhythmias were excluded from the study. Baseline clinical characteristics of the patients enrolled in this study are shown in Table I. The study was approved by the ethics committee of Fujita Health University and conformed to the principles outlined in the Declaration of Helsinki. All patients provided written informed consent.

B. Multiscale Analysis

1) Self-Similarity and Wavelets: Classical multiscale analysis relies on the estimation of wavelet coefficients, which are obtained by comparing the cumulated sum of a series of *RR* intervals $\{RR\}$ to the collection $\{\psi_{j,k}(t) = 2^{-j}\psi(2^{-j}t - k)\}_{(j,k)\in\mathbb{N}^2}$ of dilated and translated templates of a mother wavelet ψ via inner products, $d_{\{RR\}}(j,k) = \langle \psi_{j,k} | \{RR\} \rangle$ (see, e.g., [30] for details on wavelet transforms).

For *self-similar* processes $\{RR\}$ such as fractional Brownian motion, which are commonly used models for heartbeat dynamics series [19], the so-called wavelet *structure functions* $S(q, j)$ display power laws with respect to scale j and order of sample moments q:

$$S(q, j) = \sum_{k=1}^{n_j} |d_{\{RR\}}(j,k)|^q \simeq K_q 2^{jqH} \tag{1}$$

with n_j the number of $d_{\{RR\}}(j,k)$ available at scale 2^j. The Hurst parameter H and the function $S(q = 2, j)$ are directly related to the distribution of energy along frequencies (i.e., to the Fourier spectrum or autocorrelation of $\{RR\}$). They are hence linear features of $\{RR\}$ that can be efficiently estimated using wavelets [8], [10].

2) Multifractal Models and Wavelet p-Leaders: It has been demonstrated that self-similar models describe only parts of the scaling properties in HRV data and that *multifractal* models could provide more complete descriptions (see, e.g., [2], [8]). These models essentially imply that the linear scaling exponents qH in (3) should be replaced with a more flexible, concave function $\zeta(q)$, and that the parameter H alone can no longer account for all scaling properties in HRV data. To correctly estimate $\zeta(q)$, wavelet coefficients must be replaced with non-linear multiscale quantities that sense the local regularity fluctuations in data across all finer scales [10]. In this study, we employ the wavelet *p-leaders*, which have recently renewed the state-of-the-art for the estimation of multifractal models [26], for the primitive $\{RR\}'(t) = \int^t \{RR\}(s)ds$ of $\{RR\}$. They are defined as ℓ^p-norms, computed in a narrow time neighborhood over all finer scales, of the wavelet coefficients of $\{RR\}'$,

$$L^{(p)}_{\{RR\}'}(j,k) = \left(2^j \sum_{\lambda' \subset 3\lambda_{j,k}} |d_{\{RR\}'}(\lambda')|^p 2^{-j'}\right)^{1/p}, \tag{2}$$

with $\lambda_{j,k} = [k2^j, (k+1)2^j)$ and $3\lambda_{j,k} = \bigcup_{m\in\{-1,0,1\}} \lambda_{j,k+m}$. The parameter $p > 0$ must be chosen to ensure minimal regularity constraints (cf. [26] and references therein for details on multifractal analysis, beyond the scope of this contribution).

Below, we use $p = 1$, which have been shown to yield lowest variance [26]. it has been shown that the multifractal properties of $\{RR\}$ are well described by a multiscale representation consisting of the sample cumulants Cum_m of the logarithm of p-leaders $\ln L^{(p)}_{\{RR\}'}(j,\cdot)$ [10]

$$C_m(j) \equiv \mathrm{Cum}_m \ln L^{(p)}_{\{RR\}'}(j) \simeq c^0_m + c_m \ln 2^j. \tag{3}$$

In particular, the coefficients c_m are related to $\zeta(q)$ via the polynomial expansion $\zeta(q) \equiv \sum_{m\geq 1} c_m q^m/m!$ (and hence to the multifractal spectrum, cf., [10] for details). Consequently, the leading coefficients c_1 and $C_1(j)$ are closely related to H and $S(2, j)$, respectively, and constitute linear features associated to the autocorrelation of $\{RR\}$ [8], [10], while $C_2(j)$, $C_3(j)$ and $C_4(j)$ (the variance, skewness and kurtosis of $\ln L^{(p)}_{\{RR\}'}(j)$, respectively) and c_2, c_3 and c_4 (related to the multifractal properties of $\{RR\}$) are nonlinear features that capture information beyond correlation.

C. Instantaneous Autonomic Features for Multifractals

1) Point Process Models: We model the unevenly sampled *RR* interval series through inverse-Gaussian PDFs whose first-order moment (the mean $\mu_{RR}(t, \mathcal{H}_t, \xi(t))$, with $\mathcal{H}_t$ as the history of past *RR* intervals, $\xi(t)$ the vector of the time-varying parameters, and $\xi_0(t)$ the shape parameters of the inverse-Gaussian) has an autoregressive formulation. Importantly, the use of an inverse Gaussian distribution $f(t|\mathcal{H}_t, \xi(t))$ is physiologically motivated, as it models the integrate-and-fire mechanism of the cardiac contraction [25]).

The inverse Gaussian is defined as:

$$f(t|\mathcal{H}_t, \xi(t)) = \left[\frac{\xi_0(t)}{2\pi(t-u_j)^3}\right]^{\frac{1}{2}} \times \exp\left\{-\frac{1}{2}\frac{\xi_0(t)[t-u_j-\mu(t,\mathcal{H}_t,\xi(t))]^2}{\mu(t,\mathcal{H}_t,\xi(t))^2(t-u_j)}\right\} \tag{4}$$

with $j = \widetilde{N}(t)$ the index of the previous R-wave event before time t, and:

$$\mu_{RR}(t, \mathcal{H}_t, \xi(t)) = \gamma_0 + \sum_{i=1}^{p} \gamma_1(i,t)\, RR_{\widetilde{N}(t)-i} \tag{5}$$

where $\mathcal{H}_t = (u_j, RR_j, RR_{j-1}, ..., RR_{j-p+1})$, $\xi(t) = [\xi_0(t), \gamma_0(t), \gamma_1(1,t), ..., \gamma_1(p,t)]$, and $\xi_0(t) > 0$.

Since these PDFs are defined at each moment in time, it is possible to obtain an instantaneous estimate of $\mu_{RR}(t)$ at a very fine time scale (with an arbitrarily small bin size Δ), which requires no interpolation between the arrival times of two beats, therefore addressing the problem of dealing with unevenly sampled observations. This key advantage, particularly useful when dealing with multifractality, applies also for the derivation of spectral measures, following the estimation of $\mu_{RR}(t, \mathcal{H}_t, \xi(t))$.

2) Model Identification: We estimate the parameter vectors $\xi(t)$ at each time interval $\Delta = 5$ ms using a Newton-Raphson procedure to compute the local maximum-likelihood estimate [25] using observations within a time window of 90 s. Because there is significant overlap between adjacent local likelihood intervals, we start the Newton-Raphson procedure at t with the previous local maximum-likelihood estimate at time $t - \Delta$, where Δ defines the time interval shift to compute the next parameter update. We determine the optimal model order $\{p\}$ by pre-fitting the point process model to a subset of the data. Model goodness-of-fit is based on the Kolmogorov-Smirnov (KS) test and associated KS statistics. The recursive, causal nature of the estimation allows to predict each new observation, given the previous history independently at each iteration. The model and all its parameters are therefore also updated at each iteration, without priors. In other words, each test point RR_k is tested against one instance of a time-varying model trained with points $\{RR_j\}$ with $j < k$. Autocorrelation plots are also considered to test the independence of the model-transformed intervals. Once the order $\{p\}$ is determined, the initial model coefficients are estimated by the method of least squares. Extensive details on all these steps can be found in [25].

3) Feature Selection: Our framework allows for a quantitative characterization of autonomic features based on instantaneous time- and frequency-domain estimations. Time-domain indices are based on the first and the second order moments of the underlying probability structure. Namely, given the time-varying parameter set $\xi(t)$, the instantaneous estimates of mean $\mu_{RR}(t, \mathcal{H}_t, \xi(t))$, R-R interval standard deviation $\sigma^2_{RR}(t, \mathcal{H}_t, \xi(t))$, mean heart rate $\mu_{HR}(t, \mathcal{H}_t, \xi(t))$, and heart rate standard deviation $\sigma_{HR}(t, \mathcal{H}_t, \xi(t))$ can be derived at each moment in time as follows [14], [25]:

$$\sigma^2_{RR}(t, \mathcal{H}_t, \xi(t)) = \mu^3_{RR}(t)/\xi_0(t). \tag{6}$$

$$\mu_{HR(t,\mathcal{H}_t,\xi(t))} = \tilde{\mu_{RR}}^{-1} + \xi_0(t)^{-1} \tag{7}$$

$$\sigma_{HR}(t, \mathcal{H}_t, \xi(t)) = \left[\frac{2\tilde{\mu_{RR}} + \xi_0(t)}{\tilde{\mu_{RR}}\ \xi_0{}^2(t)}\right]^{1/2} \tag{8}$$

Linear power spectrum estimation allows for selection of autonomic features in the frequency domain. In particular, given the model of $\mu_{RR}(t, \mathcal{H}_t, \xi(t))$, we can compute the time-varying parametric (linear) autospectrum [14], [25] as follows:

$$\mathcal{Q}(f,t) = \sigma^2_{RR} H_1(f,t) H_1(-f,t) \tag{9}$$

where H_1 represents the Fourier transform of the γ_1 terms (see (5)). By integrating (9) in each frequency band, we compute the indices within the very low frequency (VLF = 0^+–0.04 Hz), low frequency (LF = 0.04–0.15 Hz), and high frequency (HF = 0.14–0.45 Hz) ranges, along with their ratio (LF/HF). In the end, the instantaneous feature set considered for further analyses is as follows: $\mu_{RR}(t)$, $\xi_0(t)$, $\sigma^2_{RR}(t)$, $VLF(t)$, $LF(t)$, $HF(t)$, $LF/HF(t)$. The information about the long-term, time-varying dynamics of each given instantaneous feature can then be summarized using a subset of exponents $\zeta(2)$, c_1, c_2, c_3, c_4, estimated for each range of scales $j = 1, \ldots, 8$, as well as a subset of multiscale representation $\log_2 S(2, j)$, $C_1(j)$, $C_2(j)$, $C_3(j)$, $C_4(j)$ for $j \in [j_m, j_M]$, estimated for each range of scales $j = 5, \ldots, 19$.

D. Statistical Testing and Pattern Recognition

First, from the heartbeat series, we investigated the scaling properties and predictive value in the frame of CHF for: i) heartbeat series as interpolated using the informative Point Process

model, i.e., $\mu_{RR}(t)$; ii) heartbeat series as interpolated using a standard non informative Spline-based interpolation, referred to as the Spline Interpolated time series.

The analysis is conducted using Daubechies3 wavelets.

As mentioned in *Feature Selection*, for each feature $\mu_{RR}(t)$, $\xi_0(t)$, $\sigma^2_{RR}(t)$, $VLF(t)$, $LF(t)$, $HF(t)$, $LF/HF(t)$, we considered

- α set: a subset of exponents $\zeta(2), c_1, c_2, c_3, c_4$, obtained as local slopes estimated over 4 octaves centred at $\{1.71, 3.41, 6.83, 13.7, 27.3, 54.6, 109.2, 218.5\}$ s.
- β set: a subset of multiscale representation $\log_2 S(2, j)$, $C_1(j)$, $C_2(j)$, $C_3(j)$, $C_4(j)$ for dyadic scales $2^j \in [0.21, 3495]$ s.

We then evaluated between-group differences (NS vs. SV) for every feature using bivariate non parametric statistics (Mann-Whitney test) under the null hypothesis that the between-subject medians of the two groups are equal.

Furthermore, we employed an automatic classification algorithm based on well-known SVM in order to automatically discern NS vs. SV at a single subject level. To this extent, a multidimensional point in a given feature set was considered an outlier if z-scores associated to its dimensions were greater than 2.58 (i.e., $p < 0.01$). To assess the out-of-sample predictive accuracy of the system, we adopted a Leave-One-Out (LOO) procedure based on a SVM-based classifier. Specifically, we employed a ν-SVM ($\nu = 0.5$) with a sigmoid kernel function with $\gamma = n^{-1}$, where n is equal to the number of features. Within the LOO scheme, the training set was normalized by subtracting the median value and dividing by the median absolute deviation over each dimension. These values were then used to normalize the example belonging to the test set. During the LOO procedure, this normalization step was performed on each fold.

In order to optimize the number of features to be used for the NS vs. SV classification and to provide meaningful information for the physiopathology-related discussion of results, we applied a support vector machine recursive feature elimination (SVM-RFE) procedure. Such a procedure was carried out on the training set at each LOO fold. Then, the mode of all ranks was considered for further analyses. Note that SVM-RFE includes a correlation bias reduction strategy into the feature elimination procedure [31]. All analyses were performed using Matlab (MathWorks, Natick, Massachusetts, USA) v8.4 and an additional toolbox for pattern recognition (LIBSVM [32]). Classification results are summarized as balanced recognition accuracy, sensitivity and specificity.

III. Results

Between SV and NS patients, there were no significant differences with regard to age, sex, disease severity according to New York Heart Association classification, left ventricular ejection fraction, use of beta-blockers, angiotensin-converting enzyme inhibitor, and number of ventricular premature beats per hour. NS patients exhibited higher prevalence of ischemic events, higher plasma brain natriuretic peptide, blood urea nitrogen, and creatinine, lower hemoglobin, and were treated more frequently with diuretics during Holter recording (see Table I).

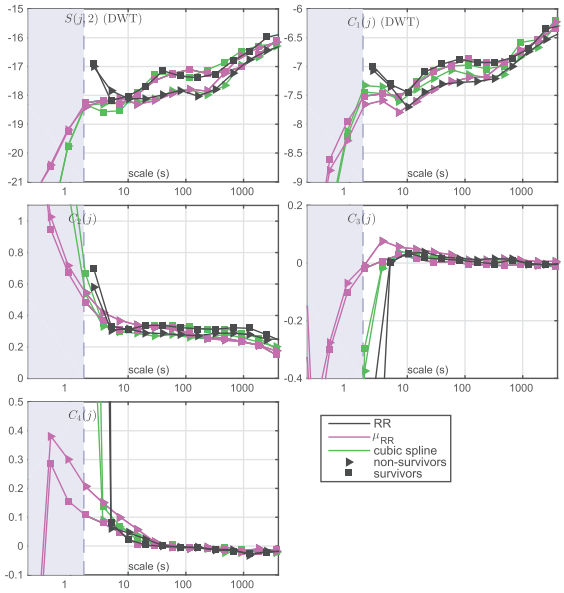

Fig. 2. Multiscale representations for the 3 different data modeling, for SV an NS subjects (median values ; the blue shaded areas indicate time scales not directly available from raw *RR* intervals).

A. Comparison Between Multifractals of Point-Process and Standard Interpolation

The wavelet coefficient-based representations $\log_2 S(2, j)$ and $C_1(j)$ (related to self-similarity) and p-leader based representations $C_2(j), C_3(j), C_4(j)$ (quantifying multifractality) for the informative point-process time series $\mu_{RR}(t)$, for non-informative cubic spline interpolation time-series, as well as for raw *RR* interval data RR, are shown in Fig. 2 as a function of scale 2^j. Scales have been translated to physical units (seconds) using the inverse of the central frequency of the wavelet. Because of the intrinsic ambiguity in the unevenly sampled raw *RR* interval series, associated scales are qualitatively matched using the average over *RR* inter-arrival times for all NS or SV subjects, respectively. This enables us to compare multiscale representations obtained from each method, as functions of equivalent scales, for NS and SV subjects. The blue shaded area indicates the finer resolution time scales that cannot be assessed for the raw *RR* interval data (for the mother wavelet used here, smaller than $\simeq 2$ s).

Results clearly show that the multiscale representations for the three time series are essentially identical at large time scales (i.e., above $\simeq 10$ s), therefore not altering actual coarse time scales. This is to be expected for the spline interpolation, and validates the proposed physiologically-informative quantification strategy.

The finer scales below ~ 2 s do not exist for original RR series but can be computed for the interpolated data. Important differences between physiologically-informative point process-derived heartbeat series and smooth deterministic spline interpolated series are shown, confirming the difference in the two approaches. For the finest two time scales of RR intervals ($\sim 2 - 10$ s), the scaling behaviour is broken and departs from that observed at intermediary ≥ 10 s. For these scales,

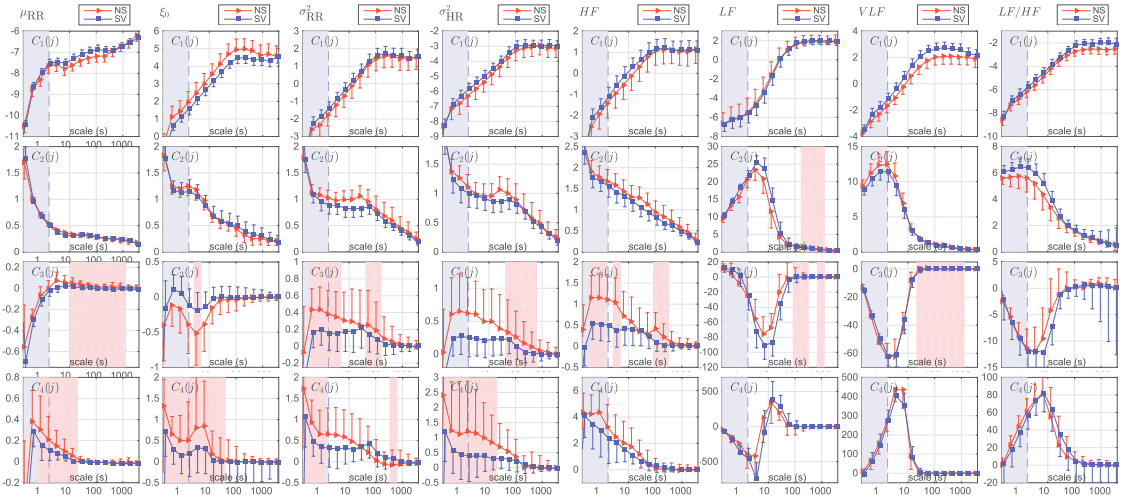

Fig. 3. Scaling and multifractal properties of physiologically-informative point process-derived series of heartbeat dynamics between SV and NS patients with severe CHF. The blue shaded areas indicate time scales not directly available from raw *RR* intervals. The red shaded areas represent scales for which statistically significant differences between SV and NS patients exist.

the spline interpolated time series show scaling in agreement with coarser scales for the (linear) self-similar representations $\log_2 S(2,\, j)$, $C_1(j)$, but they suffer from the same drawback as RR for $C_2(j)$, $C_3(j)$, $C_4(j)$.

In contrast, the physiologically-informative point-process model leads to a clean continuation of the scaling behaviour that is manifested at coarser scales for $\log_2 S(2,\, j)$, $C_1(j)$ as well as for the multifractal representations $C_2(j)$, $C_3(j)$, $C_4(j)$. This is particularly striking for $C_4(j)$, for which scaling is continued to one order of magnitude finer times scales than what can be observed on RR.

B. Scaling Properties Between CHF Survivors and Non-Survivors

The favourable comparison of the observed scale invariance properties for the informative point process-derived time-series $\mu_{RR}(t)$ motivates a closer investigation of the scaling and multifractal properties of other instantaneous estimates provided by this model. Since $S(2,\, j)$ and $C_1(j)$ quantify essentially the same information, we discard $S(2,\, j)$ here and focus on the representations $C_1(j)$, $C_2(j)$, $C_3(j)$, $C_4(j)$ for the sake of conciseness.

Fig. 3 reports these representations (from top to bottom) for the time series $\mu_{\mathrm{RR}}(t)$, $\xi_0(t)$, $\sigma^2_{RR}(t)$, $HF(t)$, $LF(t)$, $VLF(t)$, $LF/HF(t)$ (from left to right), as a function of scale. In addition, scales for which the difference between NS and SV is significant (Wilcoxon rank-sum p-values below the value 0.05) are shaded in red (uncorrected p-values). Results indicate that the time series $\mu_{RR}(t)$, $\xi_0(t)$, $\sigma^2_{RR}(t)$, $HF(t)$ display power law scaling from $\sim$0.5 s to $\sim$82 s. These scaling properties are observed both for the NS and SV groups. For $\xi_0(t)$, the shape parameter of inverse-Gaussian PDFs, scale invariance appears to be perturbed for scales $\sim 2-10$ s. Within this interval, significant discerning between SV and NS patients with CHF are associated with multifractal representations $C_3(j)$, $C_4(j)$. This is consistent with previous evidences reporting that parasympathetic activity affects complexity at short and long time scales, with maximum at precisely the range of scales $\sim 2-10$ s [33].

A second, different scaling regime is observed for coarse time scales beyond 82 s, yet is apparently non-informative for CHF clinical application, because the multiscale representations similarly converge for NS and SV. In contrast, the difference between NS and SV are almost systematically significant for finer scales for the multifractal representation $C_3(j)$, $C_4(j)$.

Importantly, such significant differences are not observed for the original RR time series. Also, interestingly, for $\xi_0(t)$, these scales with significant differences largely overlap with those where scaling is observed to be perturbed.

For the time series $VLF(t)$, $LF(t)$ and $LF/HF(t)$ of instantaneous spectral measures, scale invariance in form of power laws is evidenced exclusively for scales larger than $\sim$100 s, again both for NS and SV. This indicates that the scaling properties of combined (because of the overlap in the LF band) instantaneous sympathetic and parasympathetic activities can be considered a signature of slower physiological phenomena than those observed for the other time series. This is consistent with previous evidences reporting that sympathetic activity affects complexity only at long time scales [33], constituting best predictors of mortality following myocardial infarct or heart failure (see [33] and references therein).

These observations suggest that it is meaningful to estimate self-similar and multifractal exponents c_1 and c_2, c_3, c_4, respectively, for scales faster than $\sim$82 s for the time series $\mu_{RR}(t)$, $\xi_0(t)$, $\sigma^2_{RR}(t)$, $HF(t)$. Results are reported in Table II, together with those obtained for RR for comparison with $\mu_{RR}(t)$. The instantaneous time series $\mu_{RR}(t)$, $\xi_0(t)$, $\sigma^2_{RR}(t)$, $\sigma^2_{HR}(t)$, $HF(t)$ can be well described by a *multifractal* model since $c_m \neq 0$ for $m \geq 2$, both for NS and SV.

As discussed above, $\mu_{RR}(t)$ and RR lead to similar results, with the exception of c_4 for which $\mu_{RR}(t)$ yields a reduction of cross-subject variability by a factor 3 to 4. The time series $\xi_0(t)$, $\sigma^2_{RR}(t)$ (and to a lesser extent $HF(t)$) are further characterized by a long-range persistence type autocorrelation with $c_1 > 0.5$.

TABLE II
SCALING AND MULTIFRACTAL EXPONENTS c_1, c_2, c_3, c_4 ESTIMATED OVER SCALES [2.6, 81.9] S-MEDIAN (MED) AND MEDIAN ABSOLUTE DEVIATION (MAD)-P-VALUES FROM MANN-WHITNEY TEST

RR	NS: med	(mad)	SV: med	(mad)	p-value
c_1	0.104	(0.164)	0.156	(0.171)	0.07
c_2	−0.007	(0.049)	0.004	(0.054)	0.60
c_3	0.007	(0.040)	0.003	(0.037)	0.68
c_4	−0.045	(0.275)	−0.030	(0.298)	0.33
μ_{RR}	NS: med	(mad)	SV: med	(mad)	p-value
c_1	0.147	(0.155)	0.200	(0.175)	0.11
c_2	−0.027	(0.044)	−0.019	(0.060)	0.74
c_3	−0.019	(0.050)	−0.007	(0.048)	0.76
c_4	−0.068	(0.096)	−0.030	(0.064)	0.04
ξ_0	NS: med	(mad)	SV: med	(mad)	p-value
c_1	0.766	(0.062)	0.744	(0.095)	0.35
c_2	−0.192	(0.094)	−0.133	(0.118)	0.05
c_3	0.124	(0.254)	0.071	(0.207)	0.19
c_4	−0.340	(0.773)	−0.228	(0.423)	0.24
σ^2_{RR}	NS: med	(mad)	SV: med	(mad)	p-value
c_1	0.773	(0.058)	0.732	(0.093)	0.36
c_2	0.026	(0.120)	−0.009	(0.098)	0.23
c_3	0.016	(0.149)	0.033	(0.125)	0.91
c_4	−0.109	(0.489)	0.015	(0.538)	0.33
σ^2_{HR}	NS: med	(mad)	SV: med	(mad)	p-value
c_1	0.759	(0.066)	0.715	(0.096)	0.49
c_2	0.016	(0.118)	−0.008	(0.116)	0.24
c_3	−0.017	(0.186)	0.025	(0.164)	0.71
c_4	−0.155	(0.876)	−0.008	(0.705)	0.23
HF	NS: med	(mad)	SV: med	(mad)	p-value
c_1	0.549	(0.074)	0.526	(0.105)	0.88
c_2	−0.164	(0.122)	−0.197	(0.130)	0.19
c_3	−0.137	(0.243)	−0.080	(0.252)	0.82
c_4	−0.611	(0.883)	−0.488	(1.449)	0.35

TABLE III
CLASSIFICATION PERFORMANCES IN % USING THE α SET OF EXPONENTS ESTIMATED OVER 4 OCTAVES

Center scale (s)	Accuracy	Sensitivity	Specificity	N. Feature
1.71	63.02	46.03	80.00	3
3.41	54.05	71.43	36.67	15
6.83	58.02	79.37	36.67	28
13.7	67.90	80.95	54.84	2
27.3	**72.66**	**90.48**	**54.84**	**30**
54.6	64.52	77.42	51.61	18
109.2	57.26	72.58	41.94	2
218.5	62.90	77.42	48.39	2

Bold indicates best accuracy set.

TABLE IV
CLASSIFICATION PERFORMANCES IN % USING THE β SET

Scale (s)	Accuracy	Sensitivity	Specificity	N. Feature
0.21	60.93	44.44	77.42	15
0.43	67.95	74.60	61.29	39
0.85	68.66	85.71	51.61	28
1.71	67.90	80.95	54.84	29
3.41	66.26	84.13	48.39	29
6.83	**79.11**	**90.48**	**67.74**	**4**
13.7	63.06	80.95	45.16	12
27.3	71.86	88.89	54.84	14
54.6	58.22	80.95	35.48	17
109	64.70	77.78	51.61	11
218	63.36	42.86	83.87	1
437	71.07	87.30	54.84	31
874	61.75	42.86	80.65	1
1748	67.13	76.19	58.06	21
3495	77.44	96.83	58.06	31

Bold indicates best accuracy per feature set.

Yet, none of the exponents c_m, considered individually, can be directly translated into the clinical practice for risk stratification between NS and SV. Consistently with the fact that autonomic nervous system linear and nonlinear dynamics cannot be fully explained by a single measure only, in the next paragraph we show how to combine the aforementioned multifractal point-process measures for SV vs. NS discrimination in CHF at a single subject level.

C. SV Versus NS Classification

Leveraging on the aforementioned results performed at a group-wise level and with inferential significance only, we moved beyond statistical analysis to automatically discern SV from NS patients with CHF at a single-subject level. Scaling and multifractal features of point process-derived heartbeat dynamics are then combined throughout a nonlinear discriminant function, allowing therefore for a direct clinical translation. Following the methodology description, we considered instantaneous dynamics of $\mu_{RR}(t)$, $\xi_0(t)$, $\sigma^2_{RR}(t)$, $\sigma^2_{HR}(t)$, $VLF(t)$, $LF(t)$, $HF(t)$, $LF/HF(t)$, and condensed the information about the long-term, time-varying dynamics using the α and β sets of exponents and multiscale representations defined in Section II-D.

Throughout the LOO-SVM procedure, prediction accuracy, sensitivity and specificity in discerning SV vs. NS patients were evaluated for feature sets α and β, whose results are shown in Tables III and IV, respectively. For each scale, these tables report the best classification accuracy using a proper combination of features, as identified by the SVM-RFE algorithm. Considering the two CHF classes, accuracy of 50% is the change.

Using the subset of exponents $\zeta(2)$, c_1, c_2, c_3, c_4, an accuracy of 72.66% was obtained for exponents estimated over scales 27.3 s $\pm$ 2 octaves. Nevertheless, specificity was barely beyond the chance level (54.84%), being therefore not suitable for an actual clinical application.

Using the subset of multiscale representation $\log_2 S(2, j)$, $C_1(j)$, $C_2(j)$, $C_3(j)$, $C_4(j)$, best classification accuracy of 79.11% was obtained at scale 6.83 s, with satisfactory sensitivity of 90.48% and specificity 67.74%. The trend of classification accuracy as a function of the number of features is shown in Fig. 4. Particularly, the following four features were selected as best candidate for the prediction of survivors in patients with CHF: $\log_2 S(2, j)$, $C_3(j)$, $C_4(j)$ calculated over $VLF(t)$, and $\log_2 S(2, j)$ calculated over $LF/HF(t)$, at scale $j = 10$ ($\sim$7 s) at which the precise choice of interpolation (here, using the informative point process model) has significant impact.

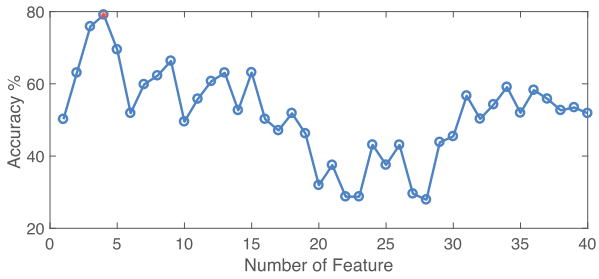

Fig. 4. Recognition accuracy in discerning NS vs. SV patients as a function of the feature rank estimated through the SVM-RFE procedure, considering feature set β comprising $\log_2 S(2,j)$, $C_1(j), C_2(j), C_3(j), C_4(j)$ at scale 6.83 s.

Merging the proposed multifractal features of α and β sets did not straightforwardly improve the aforementioned best classification accuracy of 79.11%.

IV. Discussion and Conclusion

We proposed a novel methodology combining multifractal analysis with instantaneous (time resolution of 5 ms) physiological estimates derived from inhomogeneous point-process models of cardiovascular dynamics. As previous evidences demonstrated that autonomic nervous system dynamics affects heartbeat complexity at all scales [33], we hypothesized that our methodology would provide a good predictor of mortality following congestive heart failure with single-patient specific prognostic capabilities.

All instantaneous series derived from our physiologically-informative model show a clear scaling behaviour at coarser scales over all indices of self-similarity and multifractality. Conversely, considering multifractal indices $C_2(j), C_3(j), C_4(j)$ for the scales $\sim 2-10$ s, the scaling behaviour of spline-interpolated series of *RR* intervals is broken and departs from the behaviour observed at scales $\geq$10 s. This is particularly evident for multifractal index $C_4(j)$. Note that self-similar models describe only parts of the scaling properties of the heartbeat interval series, whereas multifractal models provide a more comprehensive description (e.g., [2], [8]). Therefore, we demonstrated that scaling and multiscale representations of *RR* interval series is biased by the interpolating method employed (e.g., linear, spline, etc.). Therefore, more informative ad-hoc physiologically plausible models, such as the inhomogeneous point-process [14], [25], are strongly recommended. This result is in agreement with our previous investigations [14], [25] demonstrating that the use of an inverse-Gaussian distribution, characterized at each moment in time, inherits both physiological (the integrate-and-fire initiating the cardiac contraction [25]) and methodological information.

Additionally, we found that series of purely vagal dynamics, i.e., $HF(t)$, display power law scaling from $\sim$0.5 s to $\sim$82 s, whereas series of sympatho-vagal dynamics (e.g., $LF(t)$ and $LF/HF(t)$) are associated with scale invariance in form of power laws exclusively for scales larger than $\sim$100 s. This is also in agreement with previous evidences reporting that sympathetic activity affects complexity at long time scales [33] only. Scaling and multifractal properties of circadian heartbeat dynamics in CHF patients, therefore, do not arise at a sinus-node level, but seem to be already intrinsically present in vagal and sympatho-vagal dynamics. At a speculative level, this can be due to dysfunctional acetylcholine release on adrenergic receptors on the vagal terminals, and/or dysfunctional cytosolic adenosine 3,5-cyclic monophosphate release in post-junctions, and/or dysfunctional acetylcholine release on muscarinic receptors [1].

Using these measures, we were able to predict survivor and non-survivor CHF patients (4 year follow-up) with a satisfactory accuracy of 79.11% (sensitivity 90.48% and specificity 67.74%), considering newly-derived heartbeat variables. To the best of our knowledge, the majority of the previous studies dealing with CHF mortality prediction evaluated the predictive power of novel HRV markers using p-values and statistical inference only. Since results from statistical inference refer to a group-level analysis, whereas our classification results deal with single subject-level analysis, a proper comparison of the proposed multifractal point-process methodology with these studies cannot be performed. To give an idea of the significance of our results, here we mention few studies that quantified accuracy, specificity, and sensitivity of an HRV- based methodology for the mortality prediction in CHF. In particular, our results show higher statistical performances than Yang *et al.* (accuracy: 74.4%) [34], Bigger *et al.* (sensitivity 58%, specificity of 71%) [35], and are comparable with Pecchia *et al.* (79.3%) [36]. An indirect quantitative reference to our results with other relevant reports would point at an accuracy rate lower than Melillo *et al.* (85.4%) [37], Guidi *et al.* (86%, sensitivity and sensibility not reported) [38], and Shahbazi *et al.* (100%) [39], although Melillo *et al.*'s method is with a specificity rate of 63.6%, and results from Melillo *et al.*, Guidi *et al.*, and Shahbazi *et al.* are from 41, 50, and 44 patients, respectively. Here, it is important to highlight again that our study is associated with a significantly higher statistical power than others, given our sample of 94 patients. Also, it must be noted that methods proposed by Guidi *et al.* [38], and Yang *et al.* [34] need some parameters as input that should be gathered directly from physicians, while the adoption of only HRV measures, as in the current study, enables a completely automatic assessment.

We found that optimal predictors of mortality in this kind of pathology are associated with multifractal quantification of very low frequency oscillations ($<$0.04 Hz) of heartbeat dynamics. Although precise physiological correlates of such VLF are not well-defined yet [4], it is reasonable to associate proper diagnostic and prognostic value to multifractal changes in cardiovascular nonlinear oscillations with period between 25 s and 100 s. Accordingly, other studies involving circadian cardiovascular rhythms or long-term sleep recordings highlighted such clinical value of VLF dynamics, also as a powerful predictor of clinical prognosis in patients with CHF [40]–[44]. In particular, testing on a large cohort of asymptomatic participants undergoing 24 h Holter ECG recordings, the short-term fractal scaling exponent of heartbeat dynamics and VLF power have been recently selected as best candidate for the prediction of CHF onset on follow-up [44]. To this extent, using the same standard clinical recordings, our study makes a scientific step

forward, providing an effective methodology predicting mortality in CHF within a 4 years period at a single-patient level.

The number of subjects (94) has provided solid ground for validation of our multifractal framework. Nevertheless, we are planning a new prospective clinical trial study devoted to the collection of long-term cardiovascular data from CHF patients, including mortality follow-up evaluations. Moreover, we are aware that the classification results shown in Tables III and IV cannot be considered "optimal". While in the initial phases of this study we performed some exploratory analyses including different classifiers such as Linear and Quadratic Discriminant Classifiers, K-Nearest Neighbors, Artificial Neural Network, and others, a rigorous/unbiased comparison between classifiers would require proper parameter optimization to be performed at each step of the leave one out procedure within a nested-cross validation framework, which should also include parameter optimization for each classifier. This kind of optimization would call for a larger sample size (see limitation above) and, most importantly, is beyond the scope of this study, whose primary aim is to demonstrate that novel multifractals for inhomogeneous point-process models carry very discriminant power and are associated with prediction of CHF mortality. Indeed, the obtained accuracy, with associated specificity and sensitivity, may increase with a proper optimization of the classification algorithm. Future works will also focus on the investigation of combined scaling and multifractal analysis, and instantaneous nonlinear/complex heartbeat dynamics including time-varying bispectra [14], time-varying Lyapunov spectra [45], and time-varying monovariate and multivariate cardiac entropy [16], [46], extending therefore to higher-order statistics the recently proposed *complexity variability* framework [45] (which is currently defined through second-order moments).

In conclusion, this study poses a solid methodological basis for devising a tool capable of performing accurate assessments of CHF morbidity and sudden mortality, which still remain unacceptably high despite effective ongoing drug therapies. We suggest that, in case of severe CHF, dysfunctional, multidimensional power-law scaling of instantaneous sympatho-vagal dynamics, as estimated through physiologically-plausible probabilistic models of heartbeat generation, should be considered as a high-mortality risk factor in a 4-year follow-up.

REFERENCES

[1] K. Sunagawa *et al.*, "Dynamic nonlinear vago-sympathetic interaction in regulating heart rate," *Heart vessels*, vol. 13, no. 4, pp. 157–174, 1998.

[2] P. C. Ivanov *et al.*, "Multifractality in human heartbeat dynamics," *Nature*, vol. 399, no. 6735, pp. 461–465, 1999.

[3] C. Schäfer *et al.*, "Heartbeat synchronized with ventilation," *Nature*, vol. 392, no. 6673, pp. 239–240, 1998.

[4] U. R. Acharya *et al.*, "Heart rate variability: A review," *Med. Biol. Eng. Comput.*, vol. 44, no. 12, pp. 1031–1051, 2006.

[5] Y. Yamamoto and R. L. Hughson, "On the fractal nature of heart rate variability in humans: Effects of data length and beta-adrenergic blockade," *Amer. J. Physiol.-Regulatory, Integrative Comparative Physiol.*, vol. 266, no. 1, pp. R40–R49, 1994.

[6] T. Nakamura *et al.*, "Multiscale analysis of intensive longitudinal biomedical signals and its clinical applications," *Proc. IEEE*, vol. 104, no. 2, pp. 242–261, Feb. 2016.

[7] G. Captur *et al.*, "The fractal heart—embracing mathematics in the cardiology clinic," *Nature Rev. Cardiology*, vol. 14, pp. 56–64, 2017.

[8] M. Doret *et al.*, "Multifractal analysis of fetal heart rate variability in fetuses with and without severe acidosis during labor," *Amer. J. Perinatol.*, vol. 28, no. 4, pp. 259–266, 2011.

[9] K. Kiyono *et al.*, "Non-gaussian heart rate as an independent predictor of mortality in patients with chronic heart failure," *Heart Rhythm*, vol. 5, no. 2, pp. 261–268, 2008.

[10] H. Wendt *et al.*, "Bootstrap for empirical multifractal analysis," *IEEE Signal Proc. Mag.*, vol. 24, no. 4, pp. 38–48, Jul. 2007.

[11] H. Wendt *et al.*,, "Multiscale wavelet p-leader based heart rate variability analysis for survival probability assessment in CHF patients," in *Proc. Int. IEEE EMBS Conf.*, Chicago, USA, 2014, pp. 2809–2812.

[12] M. Costa, A. L. Goldberger, and C.-K. Peng, "Multiscale entropy analysis of complex physiologic time series," *Phys. Rev. Lett.*, vol. 89, no. 6, 2002, Art. no. 068102.

[13] D. Bansal *et al.*, "A review of measurement and analysis of heart rate variability," *Int. Conf. Comput. Autom. Eng.*, pp. 243–246, 2009.

[14] G. Valenza *et al.*, "Point-process nonlinear models with Laguerre and Volterra expansions: Instantaneous assessment of heartbeat dynamics," *IEEE T. Signal Proc.*, vol. 61, no. 11, pp. 2914–2926, Jun. 2013.

[15] R. Maestri *et al.*, "Nonlinear indices of heart rate variability in chronic heart failure patients: Redundancy and comparative clinical value," *J. Cardiovascular Electrophysiology*, vol. 18, no. 4, pp. 425–433, 2007.

[16] G. Valenza *et al.*, "Inhomogeneous point-process entropy: An instantaneous measure of complexity in discrete systems," *Phys. Rev. E*, vol. 89, no. 5, 2014, Art. no. 052803.

[17] G. Valenza *et al.*, "Estimation of instantaneous complex dynamics through lyapunov exponents: A study on heartbeat dynamics," *PloS one*, vol. 9, no. 8, 2014, Art. no. e105622.

[18] T. H. Mäkikallio *et al.*, "Fractal analysis and time- and frequency-domain measures of heart rate variability as predictors of mortality in patients with heart failure," *Amer. J. Cardiol.*, vol. 87, no. 2, pp. 178–182, 2001.

[19] K. Kiyono *et al.*, "Critical scale-invariance in healthy human heart rate," *Phys. Rev. Lett.*, vol. 93, 2004, Art. no. 178103.

[20] R. Sassi *et al.*, "Multifractality and heart rate variability," *Chaos, Interdisciplinary J. Nonlinear Sci.*, vol. 19, no. 2, 2009, Art. no. 028507.

[21] S. Dutta, "Multifractal properties of ECG patterns of patients suffering from congestive heart failure," *J. Statistical Mech., Theory Exp.*, vol. 2010, no. 12, 2010, Art. no. P12021.

[22] R. Galaska *et al.*, "Comparison of wavelet transform modulus maxima and multifractal detrended fluctuation analysis of heart rate in patients with systolic dysfunction of left ventricle," *Ann. Noninvasive Electrocardiology*, vol. 13, no. 2, pp. 155–164, 2008.

[23] J. Nolan *et al.*, "Prospective study of heart rate variability and mortality in chronic heart failure: Results of the United Kingdom heart failure evaluation and assessment of risk trial," *Circulation*, vol. 98, pp. 1510–1516, 1998.

[24] T. Mäkikallio *et al.*, "Fractal analysis and time- and frequency-domain measures of heart rate variability as predictors of mortality in patients with heart failure," *Amer. J. Cardiol.*, vol. 87, pp. 178–182, 2001.

[25] R. Barbieri *et al.*, "A point-process model of human heartbeat intervals: new definitions of heart rate and heart rate variability," *Amer. J. Physiol.-Heart Circulatory Physiol.*, vol. 288, no. 1, pp. H424–H435, 2005.

[26] R. Leonarduzzi *et al.*, "p-exponent and p-leaders, part ii: Multifractal analysis. relations to detrended fluctuation analysis." *Physica A*, vol. 448, pp. 319–339, 2016.

[27] G. Valenza *et al.*, "Point-process high-resolution representations of heartbeat dynamics for multiscale analysis: A CHF survivor prediction study," in *Proc. 37th Annu. Int. Conf. IEEE Eng. Med. Biol. Soc.*, 2015, pp. 1951–1954.

[28] G. Valenza *et al.*, "Multiscale properties of instantaneous parasympathetic activity in severe congestive heart failure: A survivor vs non-survivor study," in *Proc. 39th Annu. Int. Conf. IEEE Eng. Med. Biol. Soc.,* 2017, pp. 3761–3764.

[29] L. Citi *et al.*, "A real-time automated point-process method for the detection and correction of erroneous and ectopic heartbeats," *IEEE Trans. Biomed. Eng.*, vol. 59, no. 10, pp. 2828–2837, Oct. 2012.

[30] S. Mallat, *A Wavelet Tour of Signal Processing*. Cambridge, MA, USA: Academic press, 1999.

[31] K. Yan and D. Zhang, "Feature selection and analysis on correlated gas sensor data with recursive feature elimination," *Sens. Actuators B: Chemical*, vol. 212, pp. 353–363, 2015.

[32] C.-C. Chang and C.-J. Lin, "Libsvm: A library for support vector machines," *ACM Trans. Intell. Syst. Technol.* , vol. 2, no. 3, 2011, Art. no. 27.

[33] L. E. V. Silva *et al.*, "The role of sympathetic and vagal cardiac control on complexity of heart rate dynamics," *Amer. J. Physiol.-Heart Circulatory Physiol.*, vol. 312, no. 3, pp. H469–H477, 2017.

[34] G. Yang *et al.*, "A heart failure diagnosis model based on support vector machine," in *Proc. 3rd Int. Conf. Biomed. Eng. Informat.,* 2010, vol. 3., pp. 1105–1108.
[35] J. T. Bigger *et al.*, "Frequency domain measures of heart period variability and mortality after myocardial infarction." *Circulation*, vol. 85, no. 1, pp. 164–171, 1992.
[36] L. Pecchia *et al.*, "Remote health monitoring of heart failure with data mining via cart method on HRV features," *IEEE Trans. Biomed. Eng.*, vol. 58, no. 3, pp. 800–804, Mar. 2011.
[37] P. Melillo *et al.*, "Classification tree for risk assessment in patients suffering from congestive heart failure via long-term heart rate variability," *IEEE J. Biomed. Health Informat.*, vol. 17, no. 3, pp. 727–733, May 2013.
[38] G. Guidi *et al.*, "Heart failure artificial intelligence-based computer aided diagnosis telecare system," *Int. Conf. Smart Homes Health Telematics*, 2012, pp. 278–281.
[39] F. Shahbazi and B. M. Asl, "Generalized discriminant analysis for congestive heart failure risk assessment based on long-term heart rate variability," *Comput. Methods Programs Biomed.*, vol. 122, no. 2, pp. 191–198, 2015.
[40] L. Bernardi *et al.*, "Physical activity influences heart rate variability and very-low-frequency components in holter electrocardiograms," *Cardiovascular Res.*, vol. 32, no. 2, pp. 234–237, 1996.
[41] T. Shiomi *et al.*, "Augmented very low frequency component of heart rate variability during obstructive sleep apnea," *Sleep*, vol. 19, no. 5, pp. 370–377, 1996.
[42] M. Hadase *et al.*, "Very low frequency power of heart rate variability is a powerful predictor of clinical prognosis in patients with congestive heart failure," *Circulation J.*, vol. 68, no. 4, pp. 343–347, 2004.
[43] A. Tamura *et al.*, "Association between the severity of obstructive sleep apnea and very low frequency powers in frequency domain analysis of heart rate variability," in *Eur. Heart J.*, vol. 37, pp. 263–264, 2016.
[44] V. N. Patel *et al.*, "Association of holter-derived heart rate variability parameters with the development of congestive heart failure in the cardiovascular health study," *JACC: Heart Failure*, vol. 5, no. 6, pp. 423–431, 2017.
[45] G. Valenza *et al.*, "Complexity variability assessment of nonlinear time-varying cardiovascular control," *Sci. Rep.*, vol. 7, 2017, Art. no. 42779.
[46] G. Valenza *et al.*, "Instantaneous transfer entropy for the study of cardiovascular and cardio-respiratory nonstationary dynamics," *IEEE Trans. Biomed. Eng.*, vol. 65, no. 5, pp. 1077–1085, May 2018.